

## Analysis of time delay difference due to parametric mismatch in matched filter channels<sup>‡</sup>



Q1

Guillermo Stuarts<sup>\*,†</sup> and Pedro Julián

*Department of Electrical and Computer Engineering and Instituto de Investigaciones en Ingeniería Eléctrica (IIIE),  
Universidad Nacional del Sur - CONICET, Bahía Blanca, Argentina*

### SUMMARY

This paper presents an analysis of the time delay difference between the outputs of two matched filter channels, in the presence of parametric mismatch. A theorem for computing the cross-correlation value between two signals is developed. From the cross-correlation theorem, expressions are developed that estimate the effect of parametric mismatch in the differential time delay (DTD) for filters of arbitrary type and order and input signals of arbitrary form. The accuracy of these expressions is simulated and then demonstrated experimentally using a carefully designed setup. Filter design considerations that attempt to minimize spurious DTD in high-precision time delay estimation systems are presented. Copyright © 2014 John Wiley & Sons, Ltd.

Received 18 June 2013; Revised 21 May 2014; Accepted 29 May 2014

KEY WORDS: mismatch; matched filters; time delay difference; filter design

### 1. INTRODUCTION

The estimation of the time delay of a signal captured by spatially separated sensors plays a key role in many source localization and target tracking applications, such as communications, acoustics, geophysics, sonar systems and sensor networks [1–8]. Signal conditioning and filtering is an essential and unavoidable part in all of them, at the very first stage of the analog front-end. The use of a filter in the signal path introduces a phase shift that depends on the filter parameters. A slight difference between the filter parameters of two channels creates a frequency dependent phase difference that will be interpreted by the processing stage as a delay difference produced by a shift of the target source [9].

As an example, consider the system described in [10], where two channels (presumably identical) are used to condition the output of microphones with fourth-order switched-capacitors bandpass filters. The bandpass frequency range of these filters is from 100 to 300 Hz, and the purpose of the system is to measure the delay between the two signals with a precision of 5  $\mu$ s, which means 1° accuracy in the bearing angle estimation. However, if a 0.5% mismatch is considered in the filters cut-off frequencies, a spurious time delay of 14.81  $\mu$ s appears at the output when a single-tone signal of 200 Hz is used. Moreover, if a 90 Hz noise source is added, the spurious time delay could be as much as 38.1  $\mu$ s. This shows that for high accuracy sensor systems, even a small parameter mismatch can induce errors much higher than the targeted precision.

Parameter differences amongst devices inside an integrated circuit are much smaller than the overall process spread specifications. As such components have experienced exactly the same technological

\*Correspondence to: Guillermo Stuarts, Department of Electrical and Computer Engineering and Instituto de Investigaciones en Ingeniería Eléctrica (IIIE), Universidad Nacional del Sur - CONICET, Av. Alem 1253, Bahía Blanca, Argentina.

†E-mail: gstuarts@uns.edu.ar

Q2

<sup>‡</sup>An earlier version of this paper was presented at the 2011 EAMTA Conference and was published in its proceedings [9].



treatments, they are generally much more similar than devices made on different dies at different times in the process life cycle. However, even between matched components on the same die, parametric differences are observed. These differences, indicated with the term *parametric mismatch*, can be divided into two categories, namely *random mismatch* and *systematic mismatch* [11]. Random mismatch is generally attributable to microscopic device fluctuations, such as random dopant fluctuations [12], lithographic edge roughness [13], or grain boundary effects [14]. Systematic mismatch effects are generally associated with circuit design and/or layout imperfections. There are also some process technology related causes that can give rise to this type of mismatch, such as etch effect, lithography steps, well-proximity effects and local stress asymmetries [15, 16].

This paper presents an analysis of the time delay difference between the outputs of two matched filter channels, in the presence of parametric mismatch. The analysis begins considering a single frequency tone, which allows deriving exact expressions for the time delay difference arising when different order and type filters are used. When the signal is composed of more than one frequency tone, the outputs of the channels are different, and there is no closed expression for the time delay difference. In this case, we propose the use of the time delay that minimizes the cross-correlation between the two outputs. Closed form expressions are found that together with reasonable simplifications lead to practical design considerations. In fact, the analysis reveals that for applications requiring high accuracy, analog filtering must be restricted to very low order filters. In such cases, if further filtering is required by the application, it should be performed in the digital domain after the corresponding A/D conversion. Otherwise, the time delay to be measured will be completely overridden by the filters parametric mismatch. The results of the different analysis are experimentally demonstrated using a carefully designed setup.

## 2. TIME DELAY ANALYSIS

To begin the analysis, it is illustrative to explain the situation of a first-order low-pass filter, excited with a single-tone sinusoid. In such case, the system's frequency response has the following form:

$$H(j\omega) = a/(j\omega + b). \quad (1)$$

Therefore, the phase is given by

$$\phi = \tan^{-1}(\omega/b). \quad (2)$$

As depicted in Figure 1, let us now consider two systems, of the form (1), with a common sinusoidal  $F1$  input, namely  $u(t) = U \times \sin(\omega t)$ , where one of them suffers a variation in the value of the pole, changing from  $b$  to  $b + \Delta b$ , that is,

$$H^1(j\omega) = a/(j\omega + b) \quad (3)$$

$$H^2(j\omega) = a/(j\omega + b + \Delta b). \quad (4)$$

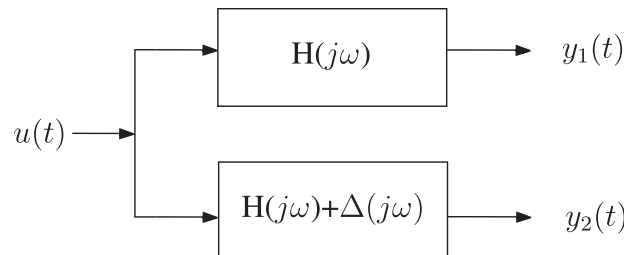


Figure 1. Setup considered with a nominal system and a perturbed system.

Accordingly, the outputs will differ in phase. Actually, both outputs will be of the following form:

$$y_1(t) = \|H^1(\omega)\| U \times \sin(\omega t + \phi_1(\omega)) \quad (5)$$

$$y_2(t) = \|H^2(\omega)\| U \times \sin(\omega t + \phi_2(\omega)). \quad (6)$$

The electronic design will try to minimize the difference between the two filters, so it makes sense to assume that  $\Delta b \ll b$  and perform a linearization of  $y_2$  as a function of  $b$ . Considering a variation  $\Delta b$  around the point  $b$ , we obtain

$$\phi_2(\omega) = \tan^{-1}(\omega/b) + (\omega/(\omega^2 + b^2)) \times \Delta b. \quad (7)$$

If we define the differential time delay (DTD) as the time difference between the two output signals, then the DTD corresponding to this system is

$$\delta(\omega) = (\phi_1(\omega) - \phi_2(\omega))/\omega = \Delta b/(\omega^2 + b^2). \quad (8)$$

Figure 2 shows a plot of  $\delta(\omega)$  versus frequency for three different values of  $b = \{1, 10, 100\}$ . In the three cases,  $\Delta b$  was chosen as a 5% variation on the nominal cut-off frequency value, that is,  $\Delta b = 0.05 \times b$ . It can be clearly appreciated that a maximum of value  $\Delta b/b^2$  occurs at low frequencies and reduces to zero as frequency increases.

The analysis can be repeated for a single pole high-pass filter to find that it has exactly the same DTD characteristics as a low-pass filter.

Notice that for both single pole filters (low-pass and high-pass), the mismatch in DTD will be small if the frequencies are close to the cut-off frequency or above it; in other words, lower frequency signals introduce larger DTD. In addition, the bigger the cut-off frequency  $\omega_o = b$ , the smaller the DTD.

### 2.1. Sensitivity analysis for general filters

According to the application, the designer may need to implement filters of higher order and different type. In multiple-pole systems, the DTD can be calculated as the sum of the DTD contributions of each

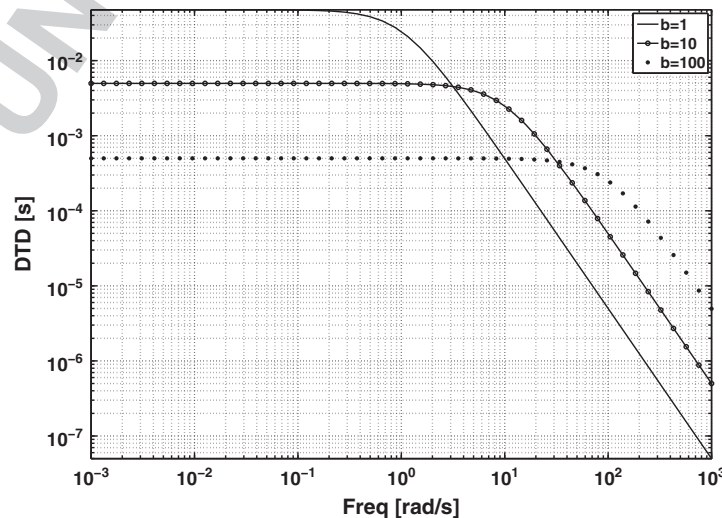


Figure 2. Differential time delay (DTD) as a function of frequency for a first-order low-pass or high-pass filter.

pole. This means that a second-order filter with a double pole at the cut-off frequency will produce a DTD twice as high as the single pole case.

Regarding filter type, a typical choice is a Butterworth filter that exhibits maximally flat magnitude response, or a Bessel filter, with maximally linear phase response, which is suitable for audio applications because it preserves the shape of the wave. Another type of filters that will be considered is the critically damped filter (CDF), in which all the poles are found at the cut-off frequency and on the real axis.

A more general expression is needed for these kinds of systems:

$$H(s) = \prod_{i=1}^N \frac{m_i s^2 + c_i s + d_i}{n_i s^2 + a_i s + b_i} \quad (9)$$

where the phase is given by

$$\varphi(j\omega) = \sum_{i=1}^N \left[ \arctan\left(\frac{c_i \omega}{d_i - m_i \omega^2}\right) - \arctan\left(\frac{a_i \omega}{b_i - n_i \omega^2}\right) \right]. \quad (10)$$

If two systems are considered, with a small variation on some of their parameters, then it is possible to derive an expression for the DTD that generalizes (8):

$$\delta(\omega) = \sum_{i=1}^N \frac{(d_i - m_i \omega^2) \Delta c_i - c_i \Delta d_i + c_i \omega^2 \Delta m_i}{(c_i \omega)^2 + (d_i - m_i \omega^2)^2} - \sum_{i=1}^N \frac{(b_i - n_i \omega^2) \Delta a_i - a_i \Delta b_i + a_i \omega^2 \Delta n_i}{(a_i \omega)^2 + (b_i - n_i \omega^2)^2}. \quad (11)$$

Figure 3 shows the DTD for 8th order Bessel, Butterworth and CDF low-pass filters with a  $F_3$  normalized cut-off frequency ( $\omega_0=1$ ) and 5% mismatch. It is possible to derive some interesting conclusions from this figure. First, the Butterworth filter gives the lowest DTD within the passband, but it peaks around the cut-off frequency, and it can cause a DTD as high as twice the low-frequency value. On the other hand, the DTD for the Bessel filter starts at a higher value but remains constant through all the passband. The CDF filter presents the highest DTD at low frequencies, but the DTD function is monotonically decreasing. As it will be shown later, this can be an advantage in system design.

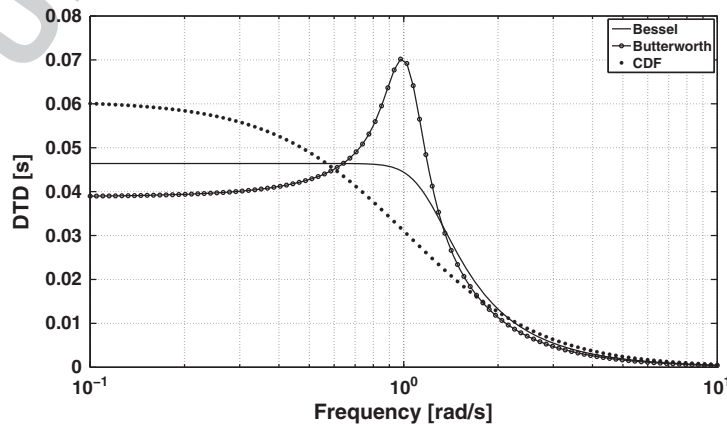


Figure 3. Differential time delay (DTD) as a function of frequency for 8th order low-pass filters with normalized cut-off frequency and 5% mismatch.

## 2.2. Analysis for several frequency components

If the input to the linear system contains more than one frequency component, and the two systems have a parametric difference, every frequency component is delayed by a different amount, and the two systems produce in general two different signals. This means that it is not possible to find a time delay  $\delta$  such that one of the outputs can be delayed to match the other. Therefore, it is necessary to introduce different criteria for DTD.

In this work, we propose the cross-correlation as the tool to define the time delay between two signals that are different. Given two signals  $s_1(t)$  and  $s_2(t)$ , the cross-correlation is defined as

$$R_{s_1, s_2}(\tau) = E[s_1(t)s_2(t - \tau)] \quad (12)$$

where  $E$  denotes expectation [1]. The argument  $\tau$  that maximizes (12) provides an estimate of the DTD, that is,

$$\delta = \operatorname{argmax} R_{s_1, s_2}(\tau). \quad (13)$$

The choice of (13) is based on the widespread use of this mathematical tool for matching closely related signals and even for estimating time delay between signals [1–4].

Without loss of generality, we consider for this case, a system like the one illustrated in Figure 1, where the input has the following form:

$$u(t) = \sum_{i=1}^N U_i \sin(\omega_i t) \quad (14)$$

then the two outputs  $y_1(t)$  and  $y_2(t)$  will be of the following form:

$$\begin{aligned} y_1(t) &= \sum_{i=1}^N \|H^1(\omega_i)\| U_i \sin(\omega_i(t + \delta_i^1(\omega_i))) + n_1(t) \\ y_2(t) &= \sum_{i=1}^N \|H^2(\omega_i)\| U_i \sin(\omega_i(t + \delta_i^2(\omega_i))) + n_2(t), \end{aligned} \quad (15)$$

where  $n_1(t)$  and  $n_2(t)$  are zero-mean and uncorrelated noise signals.

In the following, we will consider that the parametric variation is small enough such that  $\|H^1(\omega_i)\| \approx \|H^2(\omega_i)\|$ , for  $i = 1, 2, \dots, N$ , and we will note  $a_i = \|H(\omega_i)\| U_i$ . In addition, and without loss of generality, we will consider  $y_1(t)$  as reference and assume that  $\delta^1(\omega_i) = 0$ , for  $i = 1, 2, \dots, N$ , so that the individual DTD between the tones, is given by  $\delta^{(i)} \triangleq \delta^2(\omega_i) - \delta^1(\omega_i)$ .<sup>§</sup> Having introduced these considerations, we can formulate the following theorem that states the result of the cross-correlation between two outputs of the aforementioned form.

### Theorem 1

Let us consider two signals  $y_1, y_2$  formed as the sum of  $N$  tones with magnitude  $a_k$  and frequencies  $\omega_k$ , where  $\omega_k \neq \omega_n$  for  $k \neq n$  and individual differential delays  $\delta^k$ , that is,

$$y_1(t) = \sum_{k=1}^N a_k \sin(\omega_k t) + n_1(t) \quad (16)$$

$$y_2(t) = \sum_{k=1}^N a_k \sin(\omega_k(t + \delta^k)) + n_2(t) \quad (17)$$

<sup>§</sup>This notation is used for the sake of conciseness.

then, the cross-correlation between them can be approximated by

$$\hat{R}_{y_1 y_2}(\tau) = \sum_{k=1}^N \frac{a_k^2}{2} \cos(\omega_k(\tau + \delta^k)). \quad (18)$$

*Proof*

See The Appendix. ■

Using the results of Theorem 18, it is possible to approximate the DTD as the time  $\tau^*$  that maximizes (18). In fact,  $\tau^*$  is obtained from the solution of

$$\frac{\partial \hat{R}}{\partial \tau} = 0, \quad (19)$$

which is given by

$$\sum_{k=1}^N a_k^2 \omega_k \sin[\omega_k(\delta^k + \tau)] = 0. \quad (20)$$

In order to analyse the results of this theorem, it is illustrative to consider the input signal as a sum of two frequency tones and calculate the DTD between the output signals. Let

$$\begin{aligned} y_1(t) &= a_1 \sin(\omega_1 t) + a_2 \sin(\omega_2 t) + n_1(t) \\ y_2(t) &= a_1 \sin(\omega_1(t + \delta^1)) + a_2 \sin(\omega_2(t + \delta^2)) + n_2(t); \end{aligned} \quad (21)$$

according to (18), the cross-correlation between them is given by

$$\hat{R}(\tau) = a_1^2 \frac{\cos(\omega_1(\delta^1 + \tau))}{2} + a_2^2 \frac{\cos(\omega_2(\delta^2 + \tau))}{2}. \quad (22)$$

The maximum value of  $\hat{R}(\tau)$  is obtained from solving  $d\hat{R}(\tau)/d\tau = 0$  where also  $d^2\hat{R}(\tau)/d\tau^2 < 0$ , which is given by

$$\frac{a_1^2 \omega_1 \sin(\omega_1(\delta^1 + \tau))}{2} = -\frac{a_2^2 \omega_2 \sin(\omega_2(\delta^2 + \tau))}{2}. \quad (23)$$

Two cases can be considered here. Let us first examine the case where each individual delay and the solution delay are small compared to the period of the signal frequencies, that is,  $\omega_i(\tau + \delta^{(i)}) \ll 1$  for  $i = 1, 2$ .

(1) *Individual DTD small compared to  $1/\omega_i$  and  $i = 1, 2$ :* In this case, we can approximate  $\sin(\omega_i(\tau + \delta^{(i)})) \cong \omega_i(\tau + \delta^{(i)})$ , so that (23) reduces to

$$a_1^2 \omega_1^2 (\delta^1 + \tau) = -a_2^2 \omega_2^2 (\delta^2 + \tau). \quad (24)$$

A simple algebraic manipulation yields the value for  $\tau$ :

$$\tau = \alpha \delta^1 + (1 - \alpha) \delta^2 \quad (25)$$

where

$$\begin{aligned} \alpha &= \frac{\omega_1^2 a_1^2}{\omega_1^2 a_1^2 + \omega_2^2 a_2^2} \\ (1 - \alpha) &= \frac{\omega_2^2 a_2^2}{\omega_1^2 a_1^2 + \omega_2^2 a_2^2}. \end{aligned} \quad (26)$$

Several interesting conclusions can be drawn from (25). First of all, notice that the composite DTD is the convex combination of the two individual delays, thus, the DTD is always going to be an

intermediate value, that is, a value in the set

$$\Lambda = [\min(\delta^1, \delta^2), \max(\delta^1, \delta^2)]. \quad (27)$$

This means that if the filter type is such that its DTD function is monotonically decreasing, then the low-frequency DTD value can be used as an upper bound of the system DTD, for any composition of the input signal.

Secondly, notice from (26) that whether the composite DTD is closer to one delay or the other is dependent on the square of the frequency and the square of the amplitude. Therefore, for high order filters where amplitude attenuation grows faster than frequency, the relative amplitude of one tone versus the other has more influence on the composite DTD than the relative values of the frequencies.

Thirdly, notice that if the amplitudes of the tones are equivalent, then the composite DTD is closer to the individual DTD of the higher frequency signal, which is always smaller for monotonically decreasing DTD functions.

The following examples illustrate these points.

#### Example 1

Let us consider two low-pass filters of the form (3) and (4), with  $a=1$ ,  $b=1$  and  $\Delta b=0.01 \times b$ , and a signal composed by the sum of two tones  $u_1(t)=\sin(\omega_1 t)$  and  $u_2(t)=\sin(\omega_2 t)$ , where  $\omega_1=0.5$  rad/s is kept constant and  $\omega_2$  is varied over the range  $[10^{-2}, 10^2]$ . The signals at the output are of the form (21). Signal  $u_1(t)$  is low frequency, so  $a_1 \approx 1$ , whereas  $a_2 = \|H(j\omega_2)\|$ . According to (8), for a low-pass filter, the individual DTD are of the form  $\delta^{(i)} = \Delta b / (\omega^2 + b^2)$ . As the first tone is fixed,  $\delta^1 = \Delta b / (0.1^2 + b^2)$  is constant, whereas  $\delta^2 = \Delta b / (\omega_2^2 + b^2)$ .

Figure 4 shows the individual DTD and the composite DTD. It can be appreciated that at low  $\omega_2$  F4 frequencies, both amplitudes are close to unity, the individual DTD satisfies  $\delta^2 \approx \delta^1 \approx \Delta b / b^2$  so that the composite DTD is also constant and equal to  $\tau \approx \Delta b / b^2$ . In the mid-frequency range of  $\omega_2$ , we can see that the magnitude has not yet fallen appreciably, but the frequency has increased; therefore,  $\tau$  is closer to  $\delta^2$ . Eventually, the increase in frequency is compensated by the decrease in magnitude, and the composite DTD reaches an equilibrium point between  $\delta^1$  and  $\delta^2$ .

#### Example 2

Let us consider now two high-pass filters of the form  $\|H_1(\omega)\| = a_j\omega / (j\omega + b)$  and  $\|H_2(\omega)\| = a_j\omega / (j\omega + b + \Delta b)$ , with  $a=1$ ,  $b=1$  and  $\Delta b = -0.01 \times b$  and two signals of frequencies  $\omega_1=1$  rad/s,

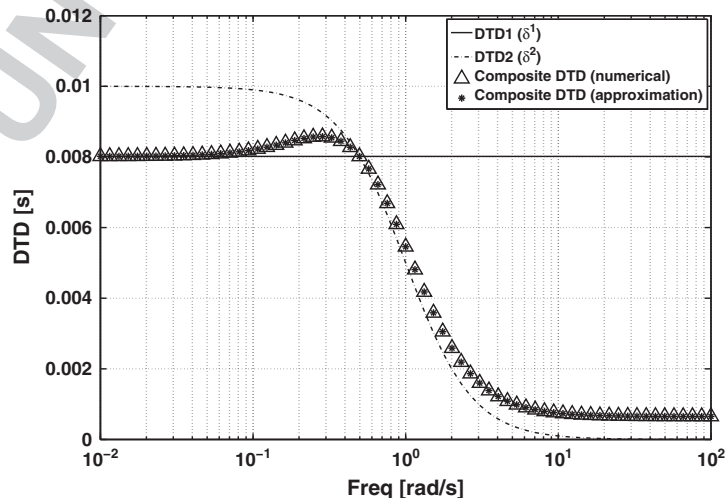


Figure 4. Individual (DTD1 =  $\delta^1$  and DTD2 =  $\delta^2$ ) and composite differential time delay (DTD) as a function of  $\omega_2$  for a first-order low-pass filter.

$\omega_2 \in [10^{-2}, 10^2]$ . In this case,  $a_i = \omega_i / \sqrt{\omega_i^2 + b^2}$ ,  $i = 1, 2$ , so that the low-frequency term is  $a_1 \approx \omega_1/b$ , and the high-frequency term is  $a_2 \approx 1$ . The individual DTD  $\delta^1$  and  $\delta^2$  are as in Example 4.

Figure 5 shows the individual and composite DTD as a function of frequency  $\omega_2$ . It can be seen that **F5** while  $\omega_1 > \omega_2$ ,  $\tau$  is closer to  $\delta^1$ . As frequency  $\omega_2$  increases,  $\tau$  approaches  $\delta^2$ .

(2). *Individual DTD large compared to  $1/\omega_i$* : In this case, we will consider the situation where one of the frequencies, for example,  $\omega_2$  is high, so that  $\omega_2(\delta^2 + \tau) \gg 1$  while the other still satisfies  $\omega_1(\delta^1 + \tau) \ll 1$ . In this case, the first term in (22) can be Taylor approximated as a constant term, in a neighbourhood of  $\tau = -\delta^1$  where it reaches its maximum value, that is,  $a_1^2 \frac{2 \cos(\omega_1(\delta^1 + \tau))}{2} \approx a_1^2/2$ ; therefore,  $\hat{R}(\tau)$  can be written as

$$\hat{R}(\tau) = \frac{a_1^2}{2} + a_2^2 \frac{\cos(\omega_2(\delta^2 + \tau))}{2}. \quad (28)$$

The second term in Eq. (28) is periodic and has maximum values on the points

$$\Gamma = -\delta^2 + 2k\pi/\omega_2, k \in \mathbb{Z}. \quad (29)$$

Because  $\hat{R}(\tau)$  has been reduced to the sum of a constant term plus a cosine function, then, it is clear that its maximum will coincide with the maximum of the cosine function that is closer to  $-\delta^1$ . If  $k$  is allowed to be a real number, the solution of (29) coincident at  $\tau = -\delta^1$  would be  $k = \omega_2(\delta^2 - \delta^1)/(2\pi)$ . Therefore, the solution is given by

$$\begin{aligned} \tau &= -\delta^2 + 2k^*\pi/\omega_2 \\ k^* &= \lceil (\omega_2(\delta^2 - \delta^1)/(2\pi)) \rceil \end{aligned} \quad (30)$$

where  $\lceil k \rceil$  stands for the ceiling function, which gives the smallest integer greater than  $k$ .

Figures 6 and 7 show the results of Examples 1 and 2 now letting  $\omega_2 \in [10^{-2}, 10^4]$  and including the **F6 F7** approximation for high frequencies.

The high-frequency behaviour of the composite DTD function needs to be treated carefully. In a low-pass filter with an input signal containing both a low-frequency and a high-frequency components, it would make sense to assume that the time delay between the outputs, if any, will be produced by the low-frequency tone, that will have much higher amplitude. However, in this example for a first-order low-pass filter, when  $\omega_2 = 400$  rad/s it produces a composite DTD of 15 ms (almost twice the DTD for the low-frequency component) even after a 52 dB attenuation. This means

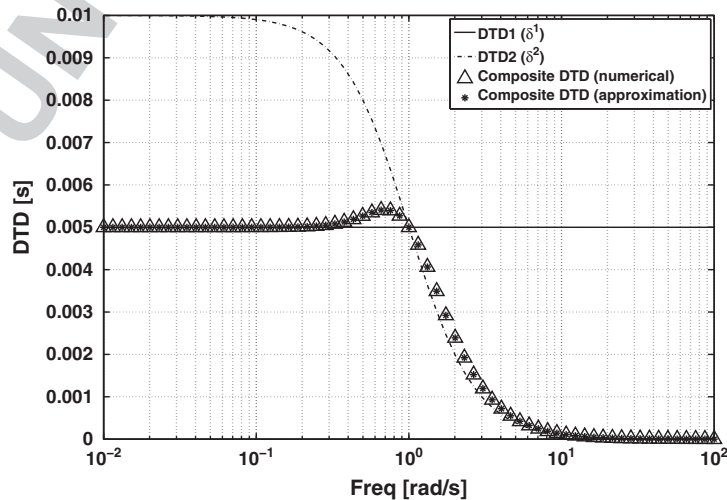


Figure 5. Individual (DTD1 =  $\delta^1$  and DTD2 =  $\delta^2$ ) and composite differential time delay (DTD) as a function of  $\omega_2$  for a first-order high-pass filter.



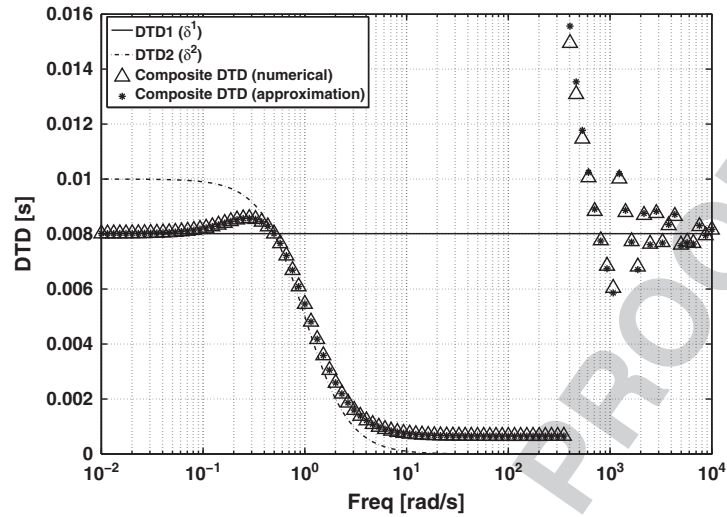


Figure 6. Individual ( $\text{DTD1} = \delta^1$  and  $\text{DTD2} = \delta^2$ ) and composite differential time delay (DTD) as a function of  $\omega_2$  for a first-order low-pass filter.

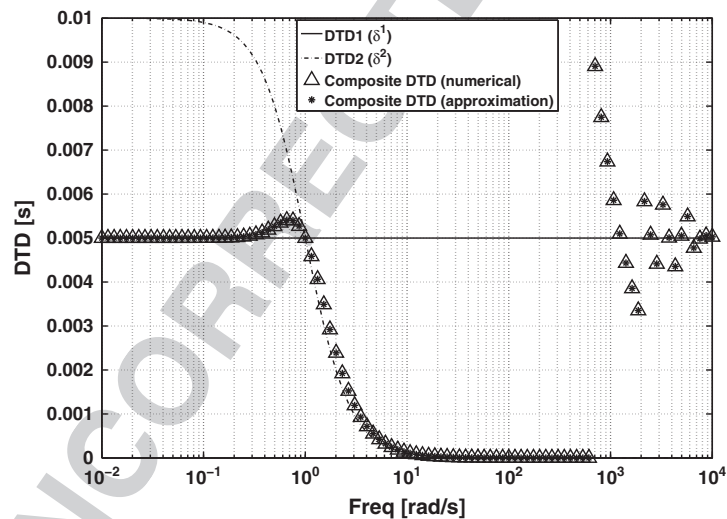


Figure 7. Individual ( $\text{DTD1} = \delta^1$  and  $\text{DTD2} = \delta^2$ ) and composite differential time delay (DTD) as a function of  $\omega_2$  for a first-order high-pass filter.

that any high-frequency noise source can significantly affect the DTD between the outputs. For this simulation, both frequency components have the same amplitude, but the same behaviour will occur if the noise source presents lower amplitude but is located closer to the sensors.

### 3. EXPERIMENTAL RESULTS

In order to validate the expressions obtained in the previous section, a set of experiments were conducted to measure the DTD in filters of different types and orders.

For the first-order measurements, RC high-pass, low-pass and bandpass filters were implemented with 1% tolerance resistors and 10% tolerance capacitors. Stanford Research Systems (SRS) SIM965 analog filters were used to implement higher order Butterworth and Bessel filters.

The input signal was generated with the SRS-DS360 low-distortion signal generator, which can provide single and dual tone signals with variable frequencies up to 200 KHz.

The acquisition is a critical step of the DTD estimation. In order to obtain a good result from the cross-correlation, at least 10 periods of the waveforms must be sampled [4]. Moreover, the sampling period must be at least 20 times smaller than the target DTD in order to have 5% accuracy. This imposes a limitation on the sampling speed and memory of the acquisition system. For example, in order to measure a DTD of  $1 \mu\text{s}$  between two 50 Hz signals, the sampling frequency needs to be higher than 20 MHz (50 ns period), and in order to acquire 10 periods of each waveform, the system must be able to store 8 million points.

For these experiments, the acquisition was performed with a Wavemaster 804Zi-A LeCroy digital oscilloscope, which allows 40 GS/s and has a memory of 20 million points per channel. The input channels, including probes, can also be a source of spurious DTD, so they need to be characterized in order to compensate their mismatch before performing any measurement. Twenty cycles of each waveform were acquired and then trimmed the data vectors from the first to the last zero-crossing, both with positive edge. Every step of the frequency sweep was measured at least 10 times, and then the resulting DTD was averaged.

The cross-correlation was performed by the *xcorr* routine in Matlab, which also requires a high amount of memory and system resources. For example, in order to run the *xcorr* routine on two vectors of 180 MB each, the system needs at least 7 GB of RAM memory.

### 3.1. High-pass RC filters

For the first-order high-pass filters, a 220 nF capacitor and a 12 K $\Omega$  resistor were used to obtain a 60 Hz cut-off frequency. Because of parametric mismatch, cut-off frequencies are different on each filter, so the frequency response of the filters had to be measured first.

The actual cut-off frequency of each filter was evaluated by means of a least-squares minimization routine in Matlab, where  $f_{c1} = 57.81 \text{ Hz}$  and  $f_{c2} = 59.44 \text{ Hz}$  were obtained. With these values, the numerical DTD was calculated and compared with the result of the cross-correlation estimation, and they are shown in Figure 8.

F8

### 3.2. Low-pass RC filters

The low-pass filters were designed to present a 20 KHz cut-off frequency; in this case, a 1 K $\Omega$  resistor and a 8.2 nF capacitor were used. The actual cut-off frequencies were measured to be  $f_{c1} = 19690 \text{ Hz}$

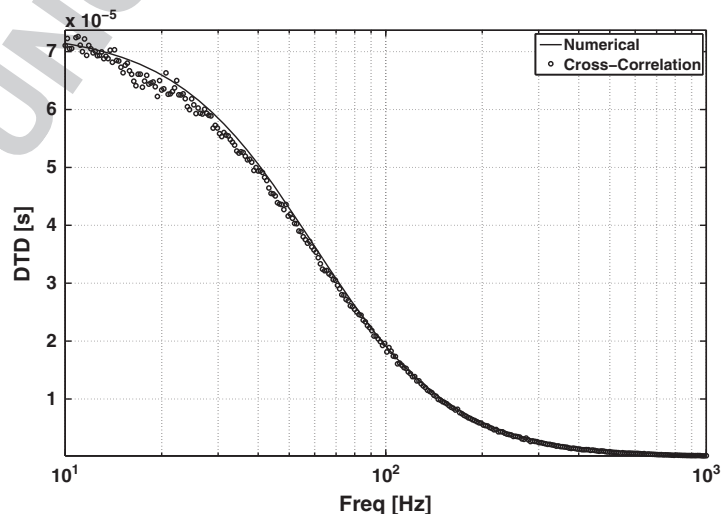


Figure 8. Differential time delay (DTD) calculated and estimated from the measurements of first-order high-pass filters.

and  $f_{c2} = 17901$  Hz. The numerical calculation of the DTD and the estimation from the cross-correlation analysis are shown in Figure 9. F9

### 3.3. Bandpass RC filters

Cascading the high-pass and low-pass filters from the previous subsections, two bandpass filters were implemented, and the results are shown in Figure 10. F10

### 3.4. Higher order filters

Depending on the application, the designer may need to implement higher order or different types of filters. A general expression for the DTD of a set of filters as a function of their parameters and mismatch was found (11). In order to validate this expression, a set of Butterworth and Bessel filters of different order were implemented as shown in Figure 11. F11

Figure 12 shows the theoretical function and the measurements for 2nd, 4th, 6th and 8th order Butterworth and Bessel low-pass filters with a cut-off frequency of 1 KHz. F12

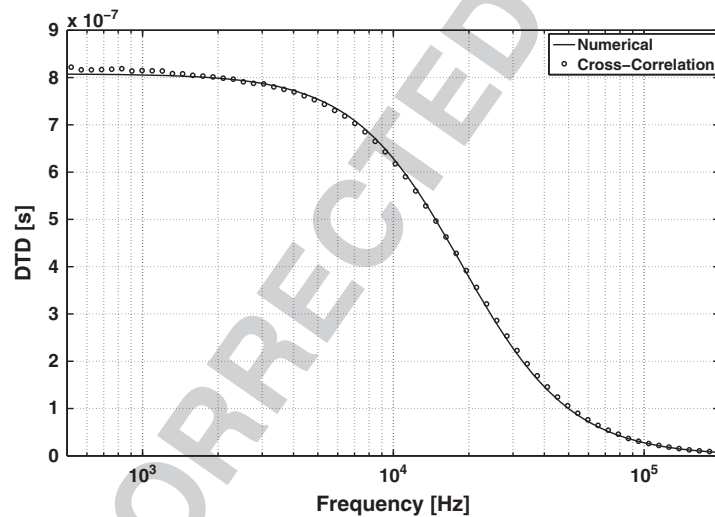


Figure 9. Differential time delay (DTD) calculated and estimated from the measurements of first-order low-pass filters.

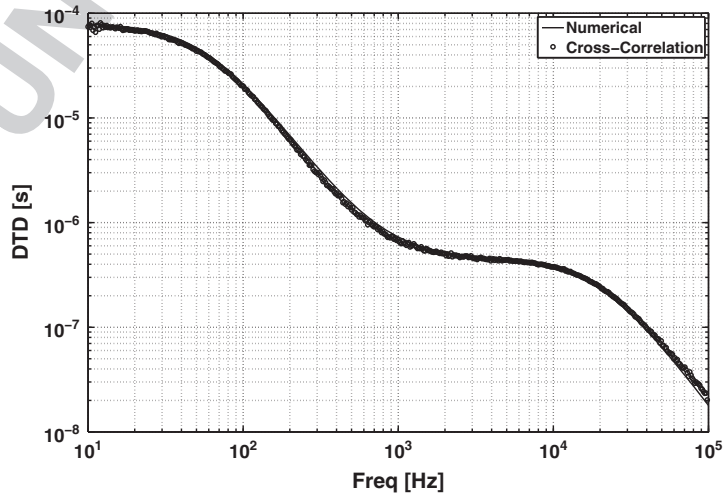


Figure 10. Differential time delay (DTD) calculated and estimated from the measurements of bandpass filters implemented as the cascade of the previous high-pass and low-pass filters.

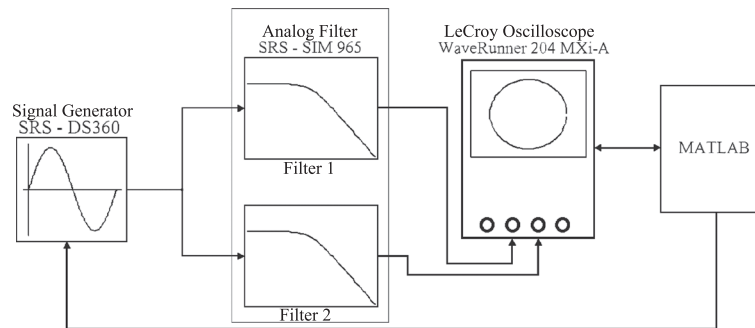


Figure 11. Filter setup used to perform the measurements.

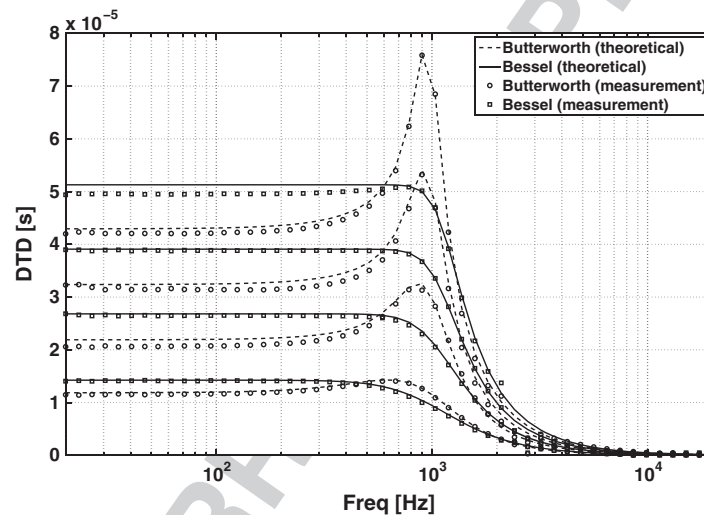


Figure 12. Theoretical and measured differential time delay (DTD) for Butterworth and Bessel low-pass filters of different orders.

Several conclusions can be drawn from Figure 12. First of all, an increase in the order of the filter produces a higher DTD. The 8th order filters show a low-frequency DTD four times higher than the value for the 2nd order case. This means that from the delay estimation perspective, it is not convenient to increase the filter order. Secondly, Butterworth filters always show a lower DTD at low frequencies than the Bessel filters. As the order increases, the difference is more appreciable. Finally, Bessel filters exhibit a monotonically decreasing DTD function, while the DTD for Butterworth filters shows a peak around the cut-off frequency.

The same conclusions hold for high-pass filters, as can be seen in Figure 13. In this case, because of the strong attenuation at low frequencies, 6th and 8th order filters show a higher error in the measured DTD.

### 3.5. Multitone input

Expressions (25) and (30) provide an estimation of the DTD when the input is a combination of two tones. In order to validate these expressions, the filter setup of Figure 11 was implemented. The input signal was constructed as the sum of a constant frequency tone  $\omega_1 = 500$  Hz and a variable frequency tone  $\omega_2$  in the range [25 and 10 KHz]. Firstly, two Butterworth second-order low-pass filters were implemented with the SIM965 filters, with cut-off frequencies of 1 and 950 Hz. Figure 14 shows the approximation and the result of the measurements of the DTD between the filter outputs.

This figure shows an important result. For second (and higher) order low-pass filters, the attenuation on the high-frequency tone is such that no periodic alternation will occur when the composite DTD converges

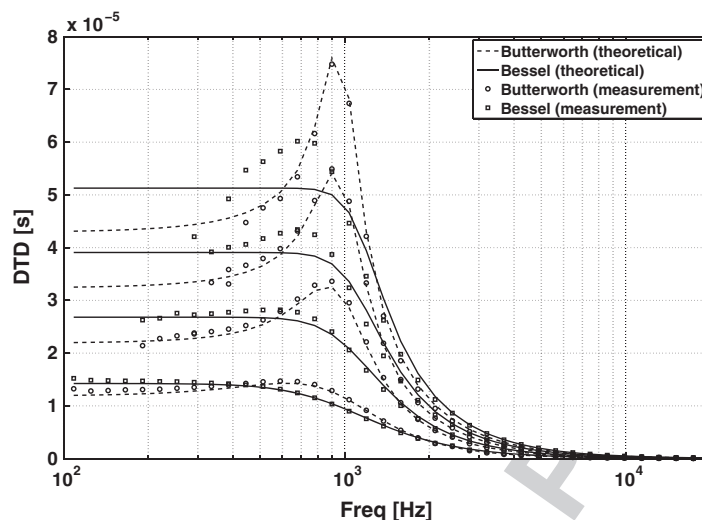


Figure 13. Theoretical and measured differential time delay (DTD) for Butterworth and Bessel high-pass filters of different orders.

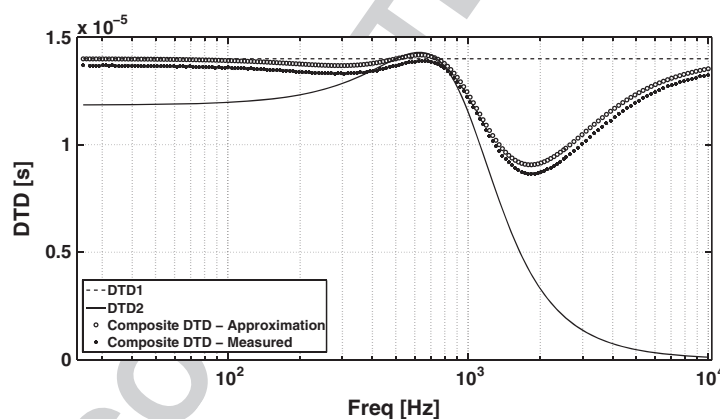


Figure 14. Differential time delay (DTD) calculated and estimated from the measurements of two second-order low-pass Butterworth filters when the input is the sum of two tones.

to the low-frequency value. In particular, for filters with monotonically decreasing DTD functions, this means that the low-frequency DTD can be used as upper bound for the composite DTD.

Secondly, two second-order high-pass Butterworth filters were implemented with the SIM965 filters, with cut-off frequencies of 500 and 450 Hz. In this case, the tone  $\omega_2$  had a variable frequency in the range [10 and 50 KHz], and the fixed tone had frequency  $\omega_1 = 300$  Hz. Figure 15 shows the approximation and the result of the measurements of the DTD between F15 the filter outputs.

For high-pass filters, increasing the filter order does not prevent the periodic alternation of the composite DTD around the DTD of the fixed tone, but it does increase the low-frequency DTD of each tone. This means that increasing the order of a high-pass filter is only prejudicial from the time delay estimation perspective.

#### 4. FILTER DESIGN

From the results obtained, we can extract the following considerations regarding filter design for signal conditioning in high-precision measurement systems.

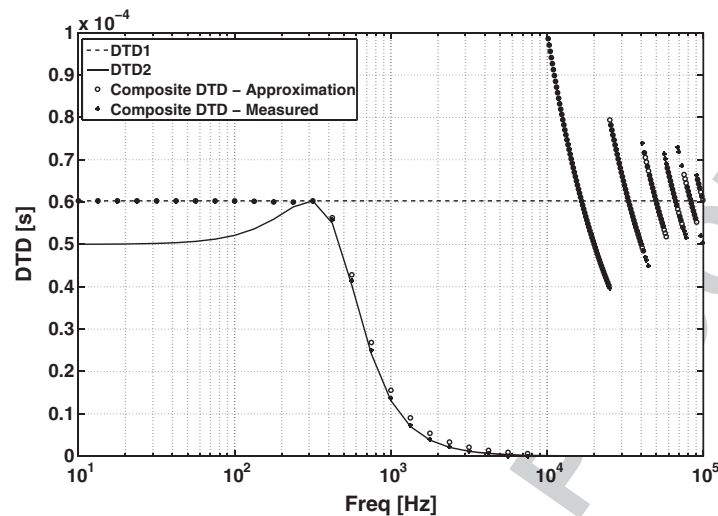


Figure 15. Differential time delay (DTD) calculated and estimated from the measurements of two second-order high-pass Butterworth filters when the input is the sum of two tones.

#### 4.1. High-pass filters

If possible, high-pass filters should be avoided in high-precision measurement systems. In a high-pass filter, the cut-off frequency needs to be lower than the frequency band of interest, and because the low-frequency DTD value is inversely related to the cut-off frequency, it will produce a high DTD that will usually act as an upper bound for the DTD of the complete system. The order of the filter acts as a multiplier of the DTD, so if a high-pass filter is unavoidable, the order should be kept as low as possible, and the cut-off frequency as close as possible to the band of interest.

In summary, for time delay applications, a high-pass filter should always be first-order and present a cut-off frequency as high as possible, even at the expense of some attenuation in the passband.

#### 4.2. Low-pass filters

Low-pass filters exhibit a similar DTD function than high-pass filters. However, the cut-off frequency is higher than the band of interest, and this means a lower low-frequency DTD (hence a lower upper bound). Again, the order of the filter needs to be kept as low as possible, but in this case, a second-order filter can prevent the periodic alternation of the DTD shown in Figures 4 and 6. It is possible to obtain the same result while preserving the low-frequency value of the first-order case if the two poles are separated by a decade. A high cut-off frequency will exhibit a lower low-frequency DTD, but it also means that signals out of the band of interest (like noise sources) will be amplified. This is a compromise for the filter designer to deal with.

In summary, a low-pass filter should always be second order, with a dominant pole setting, the cut-off frequency as high as possible, and the second pole separated by one decade.

#### 4.3. Bandpass filters

A bandpass filter can be considered as a cascade of a high-pass and a low-pass filter. As such, the DTD contribution of each filter will be added and the same design rules for the individual filters will hold. Nevertheless, if the bandwidth is high enough (that is, if the cut-off frequencies from the high-pass and the low-pass are widely separated), the DTD produced by the high-pass filter is highly dominant, and there are no design restrictions for the low-pass section.

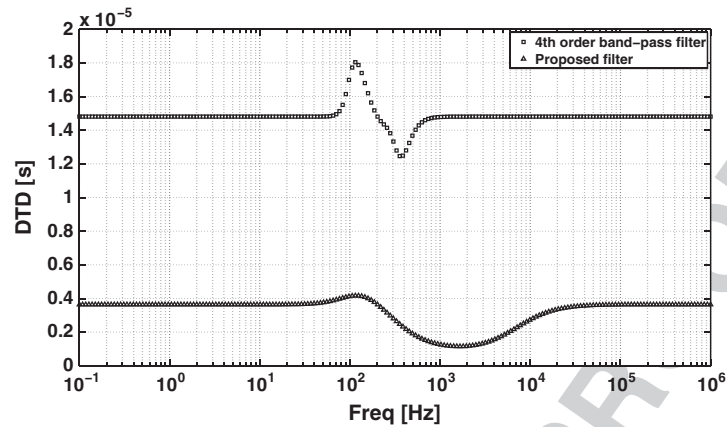


Figure 16. Differential time delay (DTD) comparison between the 4th order bandpass filter and the proposed filter, for a cut-off frequency mismatch of 0.5%.

In summary, a bandpass filter should be designed as a first-order high-pass section with cut-off frequency as high as possible, cascaded with a second-order low-pass section with cut-off frequency as high as possible and a separation of one decade between the two poles.

#### 4.4. Filter type

Butterworth, Bessel and critically damped filters were analysed in this work. Butterworth filters are a typical choice because of their maximally flat magnitude response. Regarding time delay estimation, they also produce a lower low-frequency DTD than the other filters for the same order and mismatch. However, they show a peak in the DTD function around the cut-off frequency that is increased with the order of the filter. Bessel filters have linear phase response and that translates into a flat DTD response in the passband. The DTD function is also monotonically decreasing, which means that the low-frequency DTD value can be used as an upper bound for the composite DTD of the filter. Critically damped filters show no performance improvements over Butterworth or Bessel filters.

In summary, if the application requires high order filtering, Bessel filters should be considered over Butterworth or other sharp phase response producing filters. An alternative solution would be to use low order filtering only to condition the input signals and then go through high order digital filters that will not produce any DTD between them.

#### Example 3

##### Fourth-order Bandpass filter.

We consider again the example from [10] discussed in the Introduction. The 4th order bandpass filters, with a frequency cut-off mismatch of 0.5%, will exhibit a DTD response as shown in Figure 16. For this simulation, the input signal is composed as the sum of a frequency-fixed 200 Hz tone, and a second tone with variable frequency between 0.1 and 1 MHz. In this case, the composite DTD shows a maximum of 18  $\mu\text{s}$ , and the worst possible noise scenario would produce a DTD of 38.1  $\mu\text{s}$  between the outputs.

The DTD for a second set of filters is simulated in Figure 16, designed according to the guide presented in this section. This bandpass filter consists in a first-order high-pass section with 100 Hz cut-off frequency and a second-order low-pass section with poles at 300 and 3 KHz. If the same input signal is injected to the filters and the same cut-off frequency mismatch is considered, the maximum spurious DTD is found to be 4.16  $\mu\text{s}$ , and in the worst noise scenario, the filters would produce a 10.8  $\mu\text{s}$  DTD. This means, it is possible to achieve a 4  $\times$  spurious DTD reduction just by selecting the appropriate filter setup.

## 5. CONCLUSIONS

Several expressions were developed for the estimation of time delay as a function of filter parameters. The case of a single tone going through a filter was analysed, and expression (11) was proposed as an estimation for the differential time delay between the outputs of two generalized filters of any order. Experimental and simulated results show good matching with the actual numerical calculation.

The cross-correlation between the outputs was selected as the tool to derive expressions for the estimation of the DTD when the input is a multitone signal. A set of measurements was performed on filters of different type and order to validate the results.

From the obtained results, we can conclude that for applications where the DTD between two channels is critical, the order of the signal conditioning filter must be minimized. The lowest cut-off frequency is the most critical because it produces the greatest impact on the DTD; therefore, high-pass filters should be avoided if possible or otherwise placed as close as possible to the band of interest. Low-pass filters should be second order, with cut-off frequency as high as possible, and with the two poles separated one decade. In this case, the DTD will be only slightly higher than the first-order case, and the second pole will provide enough attenuation to prevent the periodic high-frequency DTD oscillations. These results clearly suggest the need to perform the minimum required filtering at the front-end circuitry, leaving the higher order filtering for a digital stage, where filter pairs can be implemented without mismatch.

## APPENDIX

## Proof of Theorem 1

*Proof*

Let two signals  $y_1(t)$  and  $y_2(t)$ , where  $y_1(t)$  is constituted as a sum of  $N$  sinusoidal signals of magnitude  $a_k$  and frequency  $\omega_k$  ( $k = 1, 2, \dots, N$ ) and  $y_2(t)$  is such that each of its components presents a time delay  $\delta^k$  ( $k = 1, 2, \dots, N$ ) with respect to the components of  $y_1(t)$ , that is,

$$y_1(t) = \sum_{k=1}^N a_k \sin(\omega_k t) + n_1(t) \quad (\text{A1})$$

$$y_2(t) = \sum_{k=1}^N a_k \sin[\omega_k(t + \delta^k)] + n_2(t), \quad (\text{A2})$$

where  $n_1(t)$  and  $n_2(t)$  are zero-mean, uncorrelated noise signals. The cross-correlation between them is given by

$$R_{y_1, y_2}(\tau) = E[y_1(t)y_2(t + \tau)] \quad (\text{A3})$$

where  $E$  denotes expectation. Because of the finite observation time, however,  $R_{y_1, y_2}(\tau)$  can only be estimated. For ergodic processes, an estimate of the cross-correlation is given by

$$\hat{R}_{y_1, y_2}(\tau) = \lim_{T \rightarrow \infty} \frac{1}{2T} \int_{-T}^T y_1(t)y_2(t + \tau) dt \quad (\text{A4})$$

where

$$\begin{aligned} y_1(t)y_2(t + \tau) &= \sum_{k=1}^N a_k \sin(\omega_k t) \sum_{k=1}^N a_k \sin[\omega_k(t + \delta^k + \tau)] \\ &= \sum_{k=1}^N a_k^2 \sin(\omega_k t) \sin[\omega_k(t + \delta^k + \tau)] \\ &\quad + \sum_{k=1}^N \sum_{\substack{l=1 \\ l \neq k}}^N a_k a_l \sin(\omega_k t) \sin[\omega_l(t + \delta^l + \tau)] \end{aligned} \quad (\text{A5})$$



Because  $\sin(\alpha)\sin(\beta) = 1/2[\cos(\alpha - \beta) - \cos(\alpha + \beta)]$ , the second term of (A5) is

$$\begin{aligned} a_k a_l \sin(\omega_k t) \sin[\omega_l(t + \delta^l + \tau)] &= \\ &= \frac{a_k a_l}{2} \cos[(\omega_k - \omega_l)t - \omega_l(\delta^l + \tau)] \\ &\quad - \frac{a_k a_l}{2} \cos[(\omega_k + \omega_l)t + \omega_l(\delta^l + \tau)] \end{aligned} \quad (A6)$$

then

$$\begin{aligned} \int_{-T}^T a_k a_l \sin(\omega_k t) \sin[\omega_l(t + \delta^l + \tau)] dt &= \\ &= \frac{a_k a_l}{2} \int_{-T}^T \cos[(\omega_k - \omega_l)t - \omega_l(\delta^l + \tau)] dt - \frac{a_k a_l}{2} \int_{-T}^T \cos[(\omega_k + \omega_l)t + \omega_l(\delta^l + \tau)] dt \end{aligned} \quad (A7)$$

Each of the terms in (A7) is an integral of a cosine function between  $-T$  and  $T$ . Because the integral of a full period is null, its value can be bounded by the area of a cosine half cycle, which has a value of 2. Then,

$$\begin{aligned} \|E\{a_k a_l \sin(\omega_k t) \sin[\omega_l(t + \delta^l + \tau)]\}\| &= \lim_{T \rightarrow \infty} \frac{1}{2T} \left\| \int_{-T}^T a_k a_l \sin(\omega_k t) \sin[\omega_l(t + \delta^l + \tau)] dt \right\| \\ &= \lim_{T \rightarrow \infty} \frac{1}{2T} \left\| \int_{-T}^T a_k a_l \sin(\omega_k t) \sin[\omega_l(t + \delta^l + \tau)] dt \right\| \\ &\leq \lim_{T \rightarrow \infty} \frac{1}{2T} \left\| \frac{a_k a_l}{2} \int_{-T}^T \cos[(\omega_k - \omega_l)t - \omega_l(\delta^l + \tau)] dt \right\| \\ &\quad - \lim_{T \rightarrow \infty} \frac{1}{2T} \left\| \frac{a_k a_l}{2} \int_{-T}^T \cos[(\omega_k + \omega_l)t + \omega_l(\delta^l + \tau)] dt \right\| \\ &\leq \lim_{T \rightarrow \infty} \frac{1}{2T} \left\| \frac{a_k a_l}{2} 2 \right\| - \lim_{T \rightarrow \infty} \frac{1}{2T} \left\| \frac{a_k a_l}{2} 2 \right\| = 0. \end{aligned}$$

Because

$$\|E\{a_k a_l \sin(\omega_k t) \sin[\omega_l(t + \delta^l + \tau)]\}\| = 0$$

then

$$E\{a_k a_l \sin(\omega_k t) \sin[\omega_l(t + \delta^l + \tau)]\} = 0. \quad (A8)$$

On the other hand,

$$a_k^2 \sin(\omega_k t) \sin[\omega_k(t + \delta^k + \tau)] = \frac{a_k^2}{2} \cos[\omega_k(\delta^k + \tau)] - \frac{a_k^2}{2} \cos[2\omega_k t + \omega_k(\delta^k + \tau)] \quad (A9)$$

then

$$\begin{aligned} E\{a_k^2 \sin(\omega_k t) \sin[\omega_k(t + \delta^k + \tau)]\} &= E\left\{\frac{a_k^2}{2} \cos[\omega_k(\delta^k + \tau)]\right\} \\ &\quad - E\left\{\frac{a_k^2}{2} \cos[2\omega_k t + \omega_k(\delta^k + \tau)]\right\} \end{aligned} \quad (A10)$$

The second term in (A10) is of the same form as each of the terms in (A7), so

$$E\left\{\frac{a_k^2}{2} \cos[2\omega_k t + \omega_k(\delta^k + \tau)]\right\} = 0. \quad (A11)$$

For the first term of (A10), we have that

$$E\left\{\frac{a_k^2}{2} \cos [\omega_k(\delta^k + \tau)]\right\} = \lim_{T \rightarrow \infty} \frac{1}{2T} \int_{-T}^T \frac{a_k^2}{2} \cos [\omega_k(\delta^k + \tau)] dt. \quad (\text{A12})$$

Because the integrand does not depend on  $t$ , it results

$$\begin{aligned} E\left\{\frac{a_k^2}{2} \cos [\omega_k(\delta^k + \tau)]\right\} &= \lim_{T \rightarrow \infty} \frac{1}{2T} \int_{-T}^T \frac{a_k^2}{2} \cos [\omega_k(\delta^k + \tau)] dt \\ &= \frac{a_k^2}{2} \cos [\omega_k(\delta^k + \tau)] \lim_{T \rightarrow \infty} \frac{1}{2T} \int_{-T}^T dt \\ &= \frac{a_k^2}{2} \cos [\omega_k(\delta^k + \tau)] \lim_{T \rightarrow \infty} \frac{1}{2T} [T - (-T)] \\ &= \frac{a_k^2}{2} \cos [\omega_k(\delta^k + \tau)]. \end{aligned} \quad (\text{A13})$$


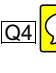
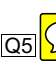
Therefore, from (A11) and (A13), it results

$$E\left\{a_k^2 \sin (\omega_k t) \sin [\omega_k(t + \delta^k + \tau)]\right\} = \frac{a_k^2}{2} \cos [\omega_k(\delta^k + \tau)] \quad (\text{A14})$$

Finally, from (A8) and (A14), we find that

$$\hat{R}_{y_1 y_2}(\tau) = \sum_{k=1}^N \frac{a_k^2}{2} \cos [\omega_k(t + \delta^k)].$$

#### REFERENCES

1. Knapp C, Carter G. The generalized correlation method for estimation of time delay. *IEEE Transactions on Acoustics, Speech, and Signal Processing* 1976; **ASSP-24**(4):320–327.
2. Azaria M, Hertz D. Time delay estimation by generalized cross correlation methods. *IEEE Transactions on Acoustics, Speech, and Signal Processing* 1984; **ASSP-32**(2):280–285.
3. Goblirsch DM, Horak DT. Error analysis of correlation methods for estimation of time delays in sensor signals. *Proceedings of the American Control Conference*, 1985; 526–529. 
4. Zou Q, Lin Z. Measurement time requirement for generalized cross-correlation based time-delay estimation. *Proceedings of the IEEE International Symposium on Circuits and Systems ISCAS 2002*, vol. **3**, 2002. 
5. Gong Y, Li L, Zhao X. Time delays of arrival estimation for sound source location based on coherence method in correlated noise environments. In 2010 Second International Conference on Communication Systems, Networks and Applications (ICCSNA), vol. **1**. IEEE, 2010; 375–378 [Online]. Available: <http://ieeexplore.ieee.org/stamp/stamp.jsp?arnumber=5588749> 
6. Erol-Kantarci M, Mouftah H, Oktug S. A survey of architectures and localization techniques for underwater acoustic sensor networks. *IEEE Communications Surveys & Tutorials* 2011; **13**(3):487–502 [Online]. Available: <http://ieeexplore.ieee.org/stamp/stamp.jsp?arnumber=5714973>
7. Shen J, Molisch A, Salmi J. Accurate passive location estimation using TOA measurements. *IEEE Transactions on Wireless Communications* 2012; **11**(6):2182–2192 [Online]. Available: <http://ieeexplore.ieee.org/stamp/stamp.jsp?arnumber=6184254>
8. He H, Wu L, Lu J, Qiu X, Chen J. Time difference of arrival estimation exploiting multichannel spatio-temporal prediction. *IEEE Transactions on Audio, Speech and Language Processing* 2013; **21**(3):463–475. [Online]. Available: <http://ieeexplore.ieee.org/stamp/stamp.jsp?arnumber=6327613>
9. Stuarts G, Julian P. Analysis of time delay difference due to parametric mismatch in matched filter channels. *2011 Argentine School of Micro-Nanoelectronics, Technology and Applications, EAMTA 2011*, Aug. 2011; 95–101.
10. Chacon-Rodriguez A, Martin-Pirchio F, Sanudo S, Julian P. A low-power integrated circuit for interaural time delay estimation without delay lines. *IEEE Transactions on Circuits and Systems II* 2009; **56**(7):575–579.
11. Tuinhout H, Wils N, Andricciola P. Parametric mismatch characterization for mixed-signal technologies. *IEEE Journal of Solid-State Circuits* 2010; **45**(9):1687–1696.
12. Stolk PA, Widdershoven FP, Klaassen DBM. Modeling statistical dopant fluctuations in MOS transistors. *IEEE Transactions on Electron Devices* 1998; **45**(9):1960–1971.
13. Croon JA, Sansen W, Maes HE. *Matching Properties of Deep Sub-Micron MOS Transistors*. Springer, 2005. ISBN:0-387-24314-3.

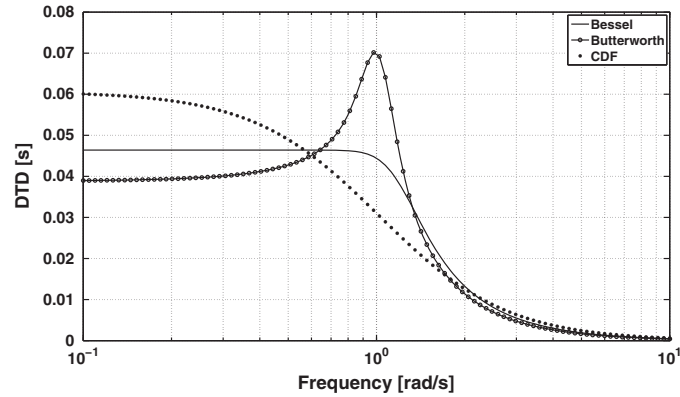
14. Tuinhout HP, Montree AH, Schmitz J, Stolk PA. Effects of gate depletion and boron penetration on matching of deep submicron CMOS transistors. In Proceedings of the International Electron Devices Meeting IEDM '97. Technical Digest. IEEE, 1997; 631–634.
15. Wils N, Tuinhout HP, Meijer M. Characterization of STI edge effects on CMOS variability. *IEEE Transactions on Semiconductor Manufacturing* 2009; **22**(1):59–65.
16. Tuinhout HP, Bretveld A, Peters WCM. Measuring the span of stress asymmetries on high-precision matched devices. *Proceedings of the International Conference on Microelectronic Test Structures ICMTS '04*, 2004; 117–122.

UNCORRECTED PROOF

## Research Article

# Analysis of time delay difference due to parametric mismatch in matched filter channels

Guillermo Stuarts and Pedro Julián



This paper presents an analysis of the time delay difference between the outputs of two matched filter channels, in the presence of parametric mismatch. Expressions are developed that estimate the effect of parametric mismatch in the differential time delay (DTD) for filters of arbitrary type and order. The accuracy of these expressions is simulated and demonstrated experimentally. Filter design considerations that attempt to minimize spurious DTD in high-precision time delay estimation systems are presented.

# Author Query Form

---

**Journal: International Journal of Circuit Theory and Applications**






**Article: cta\_2007**

Dear Author,

During the copyediting of your paper, the following queries arose. Please respond to these by annotating your proofs with the necessary changes/additions.

- If you intend to annotate your proof electronically, please refer to the E-annotation guidelines.
- If you intend to annotate your proof by means of hard-copy mark-up, please refer to the proof mark-up symbols guidelines. If manually writing corrections on your proof and returning it by fax, do not write too close to the edge of the paper. Please remember that illegible mark-ups may delay publication.

Whether you opt for hard-copy or electronic annotation of your proofs, we recommend that you provide additional clarification of answers to queries by entering your answers on the query sheet, in addition to the text mark-up.

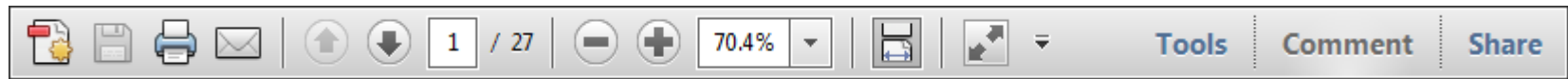
Query No.	Query	Remark
Q1	AUTHOR: Please confirm that given names and surnames/family names have been identified correctly.	
Q2	AUTHOR: This was originally reference citation [1]. It has been changed to Ref. [9] during sorting. Please check if it's ok to retain this citation here.	
Q3	AUTHOR: Please provide location of conference for Reference 3	
Q4	AUTHOR: Please provide location of symposium for Reference 4.	
Q5	AUTHOR: Please provide city location of publisher for Reference 5, 13, 14.	

USING e-ANNOTATION TOOLS FOR ELECTRONIC PROOF CORRECTION

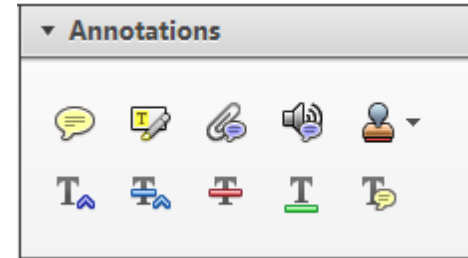
Required software to e-annotate PDFs: **Adobe Acrobat Professional** or **Adobe Reader** (version 7.0 or above). (Note that this document uses screenshots from **Adobe Reader X**)

The latest version of Acrobat Reader can be downloaded for free at: <http://get.adobe.com/uk/reader/>

Once you have Acrobat Reader open on your computer, click on the **Comment** tab at the right of the toolbar:



This will open up a panel down the right side of the document. The majority of tools you will use for annotating your proof will be in the **Annotations** section, pictured opposite. We've picked out some of these tools below:



**1. Replace (Ins) Tool – for replacing text.**

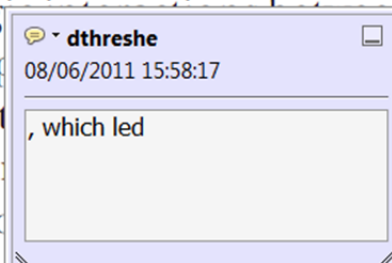


Strikes a line through text and opens up a text box where replacement text can be entered.

**How to use it**

- Highlight a word or sentence.
- Click on the **Replace (Ins)** icon in the Annotations section.
- Type the replacement text into the blue box that appears.

standard framework for the analysis of microeconomics. Nevertheless, it also led to the emergence of strategic behaviour in the number of competitors in an industry. This is that the structure of an industry, its main components and their interactions at the firm level, are exogenous to the industry. An important work on this by Shleifer and Vishny (1988) henceforth) we open the 'black b



**2. Strikethrough (Del) Tool – for deleting text.**



Strikes a red line through text that is to be deleted.

**How to use it**

- Highlight a word or sentence.
- Click on the **Strikethrough (Del)** icon in the Annotations section.

there is no room for extra profits and the number of competitors are zero and the number of firms (net) values are not determined by the number of firms. Blanchard and Kiyotaki (1987), perfect competition in general equilibrium. The effects of aggregate demand and supply in the classical framework assuming monopoly power are an exogenous number of firms

**3. Add note to text Tool – for highlighting a section to be changed to bold or italic.**



Highlights text in yellow and opens up a text box where comments can be entered.

**How to use it**

- Highlight the relevant section of text.
- Click on the **Add note to text** icon in the Annotations section.
- Type instruction on what should be changed regarding the text into the yellow box that appears.

dynamic responses of mark ups consistent with the VAR evidence

sation... y Ma... and... on n... to a... on... stent also with the demand-



**4. Add sticky note Tool – for making notes at specific points in the text.**



Marks a point in the proof where a comment needs to be highlighted.

**How to use it**

- Click on the **Add sticky note** icon in the Annotations section.
- Click at the point in the proof where the comment should be inserted.
- Type the comment into the yellow box that appears.

and supply shocks. Most of the... a... number... dard fr... cy. Nev... ole of st... ber of competitors and the imp... is that the structure of the secto



USING e-ANNOTATION TOOLS FOR ELECTRONIC PROOF CORRECTION

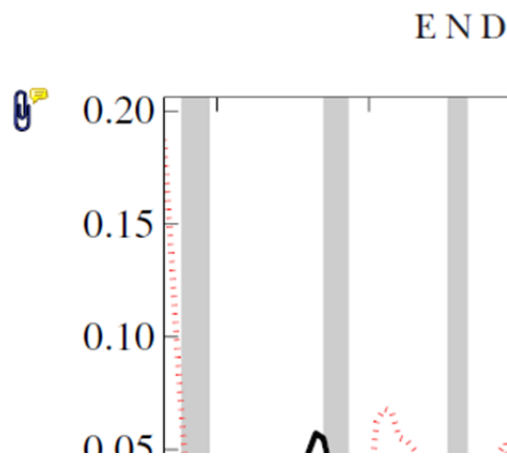
**5. Attach File Tool – for inserting large amounts of text or replacement figures.**



Inserts an icon linking to the attached file in the appropriate place in the text.

**How to use it**

- Click on the [Attach File](#) icon in the Annotations section.
- Click on the proof to where you'd like the attached file to be linked.
- Select the file to be attached from your computer or network.
- Select the colour and type of icon that will appear in the proof. Click OK.



**6. Add stamp Tool – for approving a proof if no corrections are required.**

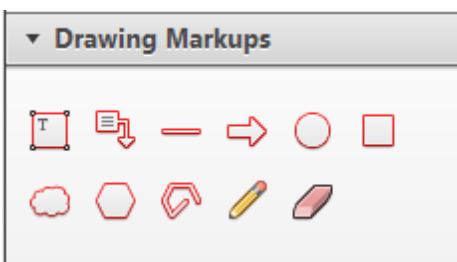


Inserts a selected stamp onto an appropriate place in the proof.

**How to use it**

- Click on the [Add stamp](#) icon in the Annotations section.
- Select the stamp you want to use. (The [Approved](#) stamp is usually available directly in the menu that appears).
- Click on the proof where you'd like the stamp to appear. (Where a proof is to be approved as it is, this would normally be on the first page).

of the business cycle, starting with the  
 on perfect competition, constant return  
 production. In this environment goods  
 extra profits and the number of firms  
 he number of firms is determined by  
 determined by the model. The New-Key  
 otaki (1987), has introduced produc  
 general equilibrium models with nomin  
 ed and supply shocks. Most of this literat

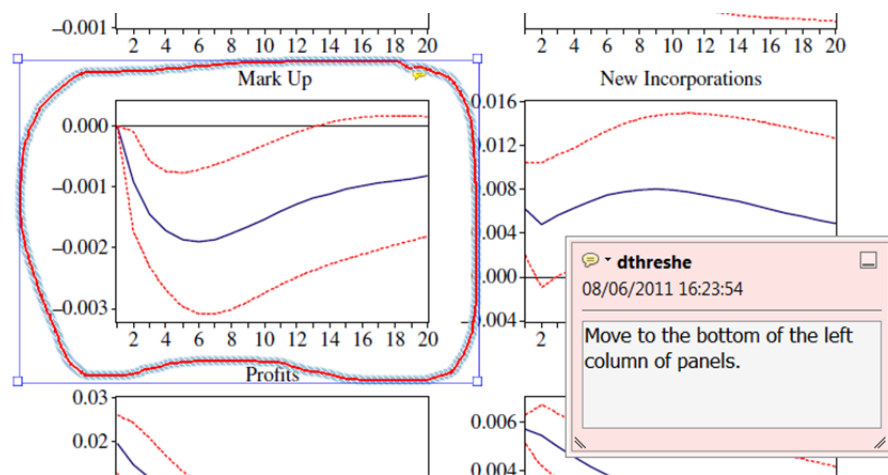


**7. Drawing Markups Tools – for drawing shapes, lines and freeform annotations on proofs and commenting on these marks.**

Allows shapes, lines and freeform annotations to be drawn on proofs and for comment to be made on these marks..

**How to use it**

- Click on one of the shapes in the [Drawing Markups](#) section.
- Click on the proof at the relevant point and draw the selected shape with the cursor.
- To add a comment to the drawn shape, move the cursor over the shape until an arrowhead appears.
- Double click on the shape and type any text in the red box that appears.



For further information on how to annotate proofs, click on the [Help](#) menu to reveal a list of further options:

